Preoperative evaluation of hepatic functional reserve following hepatectomy by technetium-99m galactosyl human serum albumin liver scintigraphy and computed tomography

Akihito Mitsumori, Isao Nagaya, Shin Kimoto, Shiro Akaki, Izumi Togami, Yoshihiro Takeda, Ikuo Joja, Yoshio Hiraki,

Department of Radiology, Okayama University Medical School, Japan

Received 20 March and in revised form 24 June 1998

Abstract. It is extremely important to have a good grasp of the acceptable limit of hepatectomy before operation because postoperative liver failure can take a fatal course; however, baseline data on the limit of hepatectomy have not been clearly defined. We therefore evaluated and compared the predicted remnant liver function obtained by computed tomography(CT) and technetium-99m diethylenetriamine penta-acetic acid-galactosyl human serum albumin (^{99m}Tc-GSA) liver scintigraphy in order to obtain precise data regarding remnant liver function before hepatectomy. We investigated 20 patients undergoing hepatectomy using the clearance rate of indocyanine green (KICG) as a parameter, and compared the predicted postoperative KICG obtained by CT and by transaxial single-photon emission tomographic (SPET) images acquired by ^{99m}Tc GSA liver scintigraphy before hepatectomy. In GSA studies, based on time-activity curves for the heart and liver, we compared HH15 (heart activity at 15 min divided by heart activity at 3 min), LHL15 (liver activcity at 15 min divided by heart plus liver activity at 15 min) and K_L (obtained from the time-activity curve for the liver) in 103 patients. In 58 patients without increased serum bilirubin, K_L was compared with KICG. In four patients, occlusion of the right portal vein was performed with the aim of carrying out secondary hepatectomy, and changes in liver volume were compared between CT and ^{99m}Tc GSA liver scintigraphy. The correlation coefficient between the postoperative KICG predicted by CT and the actual postoperative KICG was rather poor, at r = 0.569 (P<0.05); that between the postoperative KICG predicted by ^{99m}Tc GSA liver scintigraphy and the actual postoperative KICG was good, at r = 0.788 (P<0.01); correlations between K_L and HH15 and between K_L and LHL15 in 103 patients were very good or good, at r = 0.906 (P<0.001) and r = 0.807 (P<0.001), respectively, and that between K_L and KICG in 58 patients was very good, at r = 0.916 (P<0.001). In all four cases of right portal vein occlusion, the remnant liver volume ratio was markedly increased after occlusion in GSA compared with CT, and the postoperative KICG predicted by GSA after occlusion was closer to the actual postoperative KICG than that predicted by CT. It is concluded that ^{99m}Tc GSA liver scintigraphy is useful for predicting remnant liver function before hepatectomy and for evaluating changes in regional liver function after occlusion of the portal vein unilaterally.

Key words: Technetium-99m galactosyl human serum albumin – Hepatic functional reserve – Hepatic resectability – Occlusion of the unilateral portal vein – Computed tomography

Eur J Nucl Med (1998) 25:1377–1382

Correspondence to: A. Mitsumori, Department of Radiology, Okayama University Medical School, 2-5-1 Shikata-cho, Okayama-city, Okayama 700-8558, Japan

Introduction

Many patients undergoing hepatectomy have hepatocellular carcinoma (HCC); in Japan HCC is nearly always associated with liver cirrhosis (LC) or chronic hepatitis (CH), so it is essential not to exceed the limit of hepatectomy. It is extremely important to have a good grasp of the acceptable limit of hepatectomy before operation because postoperative liver failure can take a fatal course. Laboratory values such as the indocyanine green (ICG) test, prothrombin time, hepaplastin test and serum albumin level have been used for the assessment of liver function, but such values cannot provide information on the localized distribution of liver function. Moreover, baseline data on the limit of hepatectomy have not been clearly defined. On the other hand, technetium-99m diethylenetriamine-penta-acetic acid-galactosyl human serum albumin (^{99m}Tc GSA) has recently been developed as a receptor-binding ligand that specifically binds to the asialoglycoprotein receptors (ASGP-R) on the hepatocyte cell membrane. This ligand has been applied in clinical practice as one method for assessing liver function in patients with chronic and acute liver injury [1–4].

This diagnostic technique is expected to provide useful information regarding the operability and appropriate operative technique in patients with liver tumours because it can be used to evaluate the localized distribution of liver function [5]. In order to obtain precise data concerning remnant liver function before hepatectomy, we evaluated and compared the predicted remnant liver function obtained before hepatectomy by computed tomography (CT) and ^{99m}Tc GSA liver scintigraphy, using the clearance rate of ICG (KICG) (min^{-1}) as a parameter.

Materials and methods

Subjects. We studied 20 patients undergoing hepatectomy who had been admitted to Okayama University Medical School between October 1994 and March 1997: 18 patients with HCC associated with LC, one patient with haemangioma, and one patient with metastatic liver tumour from colon cancer. Seventeen were men and three were women, and their ages ranged from 45 to 68 years (mean age, 53.6 years). Subsegmentectomy was performed in five patients, monosegmentectomy in six patients, disegmentectomy in five patients, extended disegmentectomy in three patients, and trisegmentectomy in one patient. The parameter used to assess liver function was KICG. Preoperative KICG was calculated more than three times before hepatectomy, and the mean value was used. Postoperative KICG was measured 3 days after operation for comparison [6]. All patients were followed for 3–28 months after operation, and no patients died due to liver failure.

CT scanning. Prior to operation, unenhanced helical CT scanning was performed for the entire liver with 7-mm collimation at 7-mm intervals using a HighSpeed Advantage CT scanner (GE Medical Systems, Milwaukee, Wis.) during a single breath-hold. When it was difficult to detect the edges of a segment or a tumour, contrast-enhanced helical CT scanning was performed three times after the start of injection of 100 ml of iohexol (Omnipaque 300, Daiichi Pharmaceutical Co., Tokyo, Japan) via an antecubital vein at 3 ml/s in the same way as in unenhanced helical CT scanning. The first scan was begun at 30 s, the second at 70 s and the third at 180 s after the start of contrast material injection. The morphological whole liver volume was calculated from each of the images using the following formula:

$$\text{Whole liver volume} = 0.7\times \sum_{i=1}^{n} \text{Si},$$

where Si = ares in each image.

In the same way, the postoperative remnant liver volume and the tumour volume were obtained. Preoperative KICG was obtained, and the postoperative KICG predicted by CT was calculated by the following formula:

$$\text{postoperative KICG} = \text{preoperative KICG} \cdot \frac{\text{remnant liver volume}}{\text{whole liver volume} - \text{tumour volume}}.$$

^{99m}Tc GSA liver scintigraphy. All 20 patients received a single dose of 3 mg of ^{99m}Tc GSA intravenously. After the injection of 185 MBq (5 mCi) of ^{99m}Tc GSA, dynamic imaging was performed with the patient in the supine position using a GCA-7200 A/DI (Toshiba Medical Systems, Tokyo, Japan) large-field-of-view gamma camera with a low-energy, high-resolution parallel-hole collimator, and data were processed by means of a GMS-5500 A/DI (Toshiba Medical Systems, Tokyo, Japan). Computer acquisition of gamma camera data was started immediately prior to the injection of ^{99m}Tc GSA and was stopped 25 min later. Digital images (128×128 matrix) were acquired in byte mode at a rate of 15 s/frame. Hepatic single-photon emission tomography (SPET) images were acquired after the dynamic study. Each set of projection data was obtained in a 128×128 matrix, and 60 projections were acquired (6° steps, 15 s/projection). A Butterworth filter was used as the pre-reconstruction filter, and final reconstruction was performed with a Ramp filter. Attenuation correction was performed with Chang's first-order compensation procedure, and a value of 0.12 cm^{-1} was used as the effective attenuation correction coefficient. The pixel slice thickness along the axis was 6.9 mm. A cut-off level of 39% was used because results closest to the true volume were obtained using this value in an earlier phantom study [7]. In patients with accumulation in the gallbladder, we set the region of interest (ROI) so that it contained the gallbladder and subtracted it from transaxial images before the measurement of functional liver volume. After calculation of the functional whole liver volume, a cut line was entered into each section of the transaxial SPET image and the functional remnant liver volume was calculated.

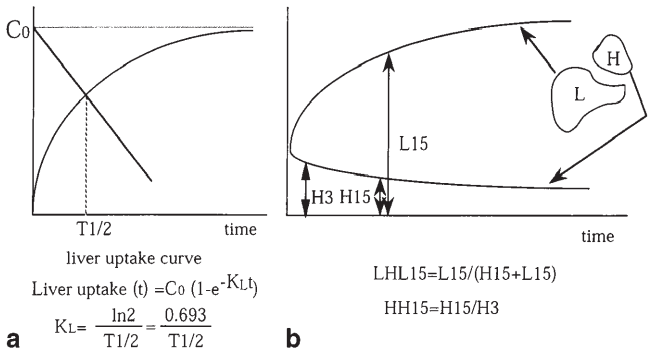

Fig. 1. Methods of scintigraphic data analysis. **a** K_L, **b** HH15, LHL15

Time-activity curves for the heart and liver were generated from ROIs for the whole liver and the precardiac region. K_L was obtained from the time-activity curve for the liver (Fig. 1a) [8, 9]. The hepatic uptake ratio of ^{99m}Tc GSA (LHL15) was calculated after the injection of ^{99m}Tc GSA by dividing the liver activity at 15 min (L15) by heart plus liver activity at 15 min (H15+L15) (Fig. 1b). The value of HH15 was calculated by dividing the heart activity at 15 min (H15) by heart activity at 3 min (H3) after the injection of ^{99m}Tc GSA (Fig. 1b).

The postoperative KICG predicted by ^{99m}TC-GSA was calculated by the following formula:

$$\text{Postoperative KICG} = \text{preoperative KICG} \cdot \frac{\text{remnant liver volume}}{\text{whole liver volume}}.$$

The postoperative KICG predicted by CT and the actual postoperative KICG were compared, as were the postoperative KICG predicted by ^{99m}Tc GSA liver scintigraphy and the actual postoperative KICG. In 103 patients K_L, was compared with HH15 and LHL15. In 58 patients without increased serum bilirubin, K_L was compared with KICG.

Portal vein occlusion. Occlusion of the portal vein unilaterally is performed with the aim of carrying out secondary hepatectomy following compensatory morphological and functional hypertrophy of the remaining lobes. In four patients, other than the 20 patients above, occlusion of the right portal vein was performed.

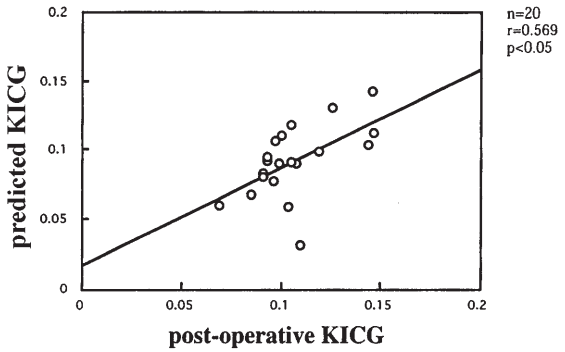

Fig. 2. Correlation between postoperative KICG and KICG predicted by CT

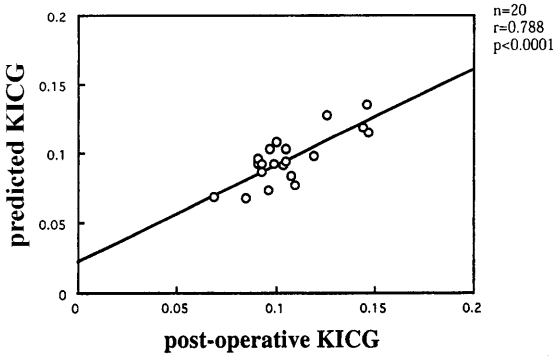

Fig. 3. Correlation between postoperative KICG and KICG predicted by GSA

Liver volume was measured 2–3 weeks after occlusion of the right portal vein by CT and ^{99m}Tc GSA liver scintigraphy at the same time. Changes in liver volume were compared between CT and ^{99m}Tc GSA liver scintigraphy.

Results

The postoperative KICG predicted by CT and the actual postoperative KICG are shown in Fig. 2. The correlation was rather poor, with the correlation coefficient $r = 0.569$ ($P<0.05$). The postoperative KICG predicted by GSA and the actual postoperative KICG are shown in Fig. 3. The correlation was good, with the correlation coefficient $r = 0.788$ ($P<0.01$). K_L and HH15 are shown in Fig. 4; the correlation was very good, at $r = 0.906$ ($P<0.001$). K_L and LHL15 are also shown Fig. 4; the correlation was good, at $r = 0.807$ ($P<0.001$). K_L and KICG are shown in Fig. 5; the correlation was very good, at $r = 0.916$ ($P<0.001$). After occlusion of the right portal vein, liver uptake was markedly decreased below the cut-off level around the liver tumour in the right lobe and an area of increased tracer accumulation was noted in the left lobe on ^{99m}Tc GSA liver scintigraphy. However, atrophic changes in the right lobe and compensatory morphological hypertrophy of the left lobe were not so evident on CT as on ^{99m}Tc GSA liver scintigraphy (Fig. 6).

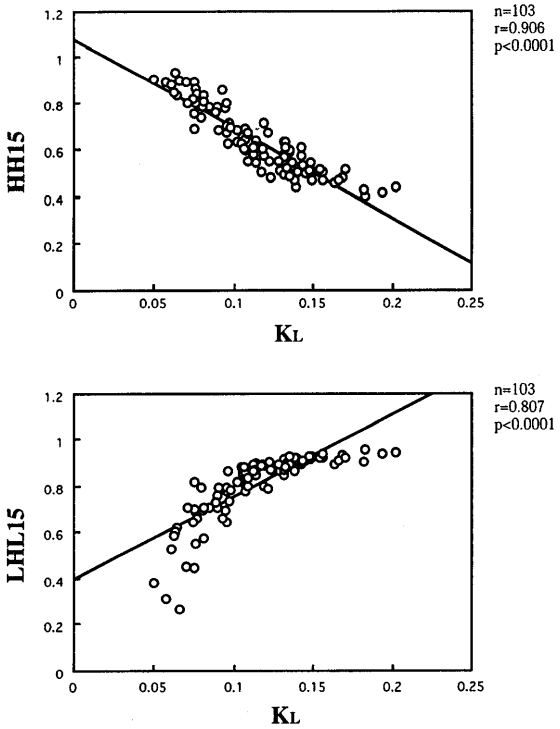

Fig. 4. Correlation between K_L and HH15 (*above*), LHL15 (*below*) in 103 patients

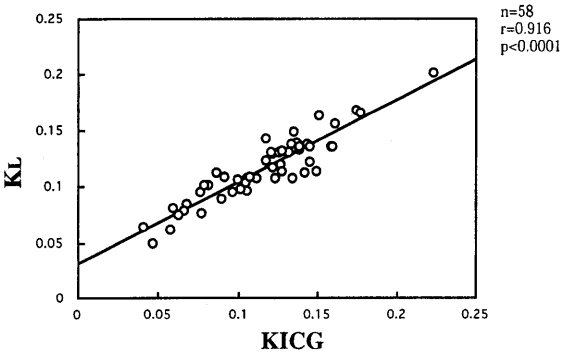

Fig. 5. Correlation between KICG and K_L in 58 patients

Table 1. Summary of four cases of portal vein occlusion

		Predicted remnant liver volume	Remnant liver volume ratio	Predicted KICG	Postoperative KICG
Case 1	CT	305→318	0.36→0.33	0.059	
	GSA	298→429	0.31→0.46	0.083	0.109
Case 2	CT	497→559	0.30→0.34	0.056	
	GSA	512→579	0.34→0.48	0.78	0.112
Case 3	CT	427→673	0.28→0.39	0.060	
	GSA	565→841	0.40→0.55	0.069	0.069
Case 4	CT	344→499	0.28→0.39	0.059	
	GSA	421→605	0.37→0.78	0.092	0.104

Figures to the left and right of the arrows refer to the situation before and after portal vein occlusion, respectively

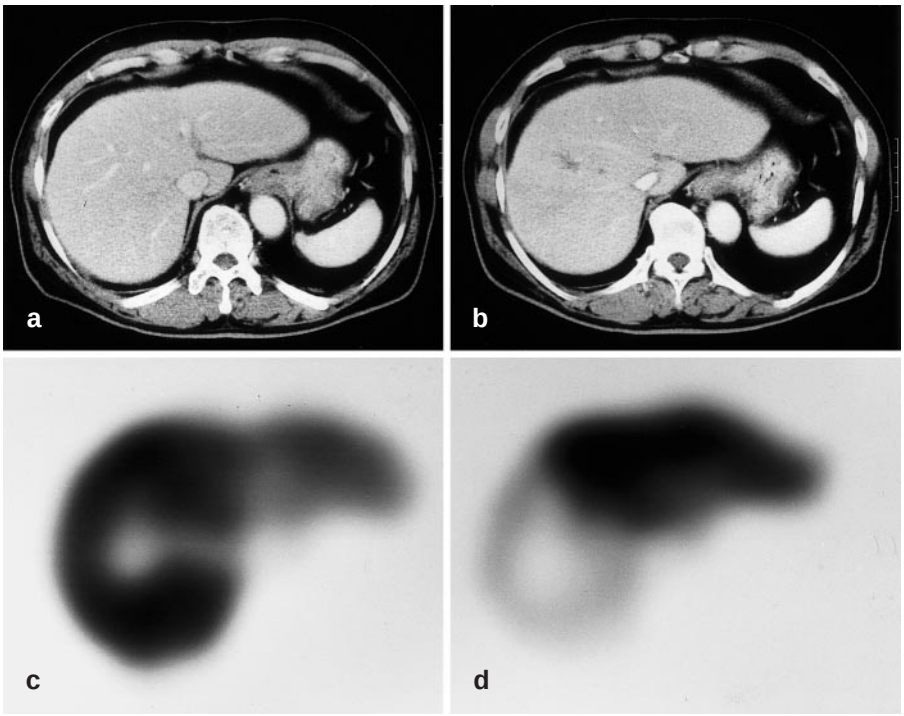

Fig. 6a–d. A 61-year-old man with CC treated with right portal vein occlusion. **a, c** Before occlusion; **b, d** after occlusion. After occlusion of the right portal vein, liver uptake was markedly decreased below the cut-off level in the right lobe and an area of increased tracer accumulation was noted in the left lobe on ^{99m}Tc GSA liver scintigraphy; atrophic changes in the right lobe and compensatory morphological hypertrophy of the left lobe were not as marked on CT as on ^{99m}Tc GSA liver scintigraphy

Details regarding the four cases of portal vein occlusion are summarized in Table 1. In all cases, the remnant liver volume ratio [CT study: remnant liver volume/(whole liver volume –tumour volume); GSA study: remnant liver volume/whole liver volume] was markedly higher after occlusion of the right portal vein in GSA as compared with CT, and the postoperative KICG predicted by GSA after occlusion was closer to the actual postoperative KICG than that predicted by CT.

Discussion

Due to advances in CT hardware, liver volume can now be calculated easily and accurately. There have been many reports concerning the evaluation of liver function based on morphological liver volume determined using CT with or without the combination of other parameters of liver function [10–12]. However, several reports have concluded that CT simply reflects morphological volume, so it is dangerous to estimate liver function by CT [13].

^{99m}Tc GSA is a newly developed receptor-binding ligand that specifically binds to the ASGP-R on the cell membrane of hepatocytes. The uptake of ^{99m}Tc GSA is an independent biochemical process and allows direct estimation of the functioning hepatocyte mass [14]. ^{99m}Tc GSA liver scintigraphy has therefore been recognized to be the best method for evaluating liver functional reserve, and it can be used to estimate regional hepatic function [13, 15, 16].

Several methods for determining the hepatic functional volume with ^{99m}Tc colloid [17, 18], ^{99m}Tc *N*-pyridoxyl-5-methyltryptophan (^{99m}Tc PMT) [19], and ^{99m}Tc DTPA human serum albumin (^{99m}Tc HSA) [20] have been reported. ^{99m}Tc PMT is a hepatobiliary imaging agent, but with this agent it is difficult to obtain satisfactory SPET images for volume measurement because it is excreted rapidly into the biliary system. ^{99m}Tc HSA is a vascular imaging agent, and does not reflect hepatocyte function. ^{99m}Tc-colloid scintigraphy mainly reflects the reticuloendothelial system and is dependent on the function of the Kupffer cells and on effective liver blood flow. ^{99m}Tc GSA, on the other hand, is taken up only by functioning hepatocytes, and its distribution in the liver is not dependent on liver blood flow [21, 22]. Torizuka et al. [21] reported that there was a discrepancy in tracer distribution between ^{99m}Tc GSA and ^{99m}Tc colloid in 18% of cases, and they speculated that there may be a difference in distribution between Kupffer cells and hepatocytes. Shuke et al. [23] reported that all of the parameters obtained from ^{99m}Tc GSA imaging showed a statistically significant correlation with the results of hepatic function tests, unlike the parameters obtained from ^{99m}Tc Sn colloid and ^{99m}Tc PMT imaging. For these reasons, ^{99m}Tc colloid scintigraphy might not precisely reflect liver function, so we should use ^{99m}Tc GSA scintigraphy to evaluate liver function. In addition, many prior studies have reported that some parameters obtained from ^{99m}Tc GSA liver scintigraphy are strongly correlated with previously identified indicators of hepatic function and that these are useful for assessing hepatic function [4, 13, 24–26]. It is not so accurate to measure the remnant liver volume using planar images obtained by ^{99m}Tc GSA scintigraphy, but by setting a cut line on each section of the transaxial SPET image, it is

possible to obtain measurements easily and accurately [15].

In this study, GSA showed better correlations than CT due to a number of factors:

1. Most of the patients who had HCC also had LC, and the degree of hepatic dysfunction in the segment or lobe containing the HCC was greater than that in the segment or lobe without HCC.
2. Liver parenchyma around the tumour was damaged by mechanical compression.
3. Secondary liver damage may have occurred due to compression of the vessels and bile ducts by the tumour.

Comparing CT and SPET images obtained using ^{99m}Tc GSA hepatic scintigraphy, we found that the defect seen on SPET images was larger than the tumour size seen on CT. This discrepancy was probably due to the factors cited above.

Previous studies revealed the risk of evaluating remnant liver function based on the morphological remnant liver volume ratio, as well as the discrepancy between function and morphology. The prediction of remnant liver function by CT is not valid because CT cannot distinguish between normal and cirrhotic or non-functioning liver tissue. We should therefore predict remnant liver function using ^{99m}Tc GSA scintigraphy rather than CT. In this study, good correlations were also obtained by functional evaluation. However, since most patients present with diffuse liver parenchymal damage, it is difficult to predict the regeneration of unresected liver tissue, even by ^{99m}Tc GSA scintigraphy. The degree of regeneration is highly dependent on the remnant liver volume ratio and the degree of impairment of remnant liver function, so the degree of functional regeneration differs from patient to patient. But when the resection area is known beforehand, it might be possible to predict the degree of regeneration by assessing the degree of hepatic dysfunction compared with the normal liver.

The effects of occlusion of the right portal venous branch revealed a remarkable degree of discrepancy between CT and ^{99m}Tc GSA liver scintigraphy. In all four patients, the remnant liver volume ratio was higher with GSA than with CT before occlusion, and 2–3 weeks after occlusion it was markedly increased with GSA as compared with CT. In all patients the postoperative KICG predicted by GSA after occlusion was closer to the actual postoperative KICG than that predicted by CT. Because focal dysfunction following portal venous occlusion does not result in immediate morphological changes, it is only in the long term that morphological changes such as atrophy or compensatory hypertrophy reflect focal liver function. If comparison is made 3–4 months after occlusion, the discrepancy is not so great, but GSA permits evaluation before morphological changes appear in CT (2–3 weeks after occlusion), reducing the risk that the tumour (especially HCC) will progress due to an increase in arterial blood flow after portal venous occlusion as well as the risk that changes in the draining vein from the portal vein to the hepatic vein will promote hematogenous metastasis [27]. However, since regeneration of the contralateral lobe after occlusion is dependent on the degree of fibrosis and the effective blood flow, these factors must be considered when deciding whether portal venous occlusion is indicated.

At our centre, on the basis of a previous study on hepatectomy, operation is indicated when the predicted KICG of the remnant liver is more than 0.07 and is contraindicated when it is less than 0.06. Whether hepatectomy is indicated is decided upon taking into account the results of hepatic function tests other than KICG, but KICG is the most important factor. For KICG values between 0.06 and 0.07, indications for hepatectomy include secondary hepatectomy after unilateral occlusion of the portal vein is investigated considering the possibility of other types of treatment (e.g. percutaneous ethanol injection, transarterial embolization and so on) and the need for aggressive therapy.

In this study, KICG was used as the parameter of liver function, but bilirubin is a competitive inhibitor of ICG, so in patients with increased serum bilirubin such as those with obstructive jaundice, the ICG test does not accurately reflect liver function. On the other hand, GSA does not compete with bilirubin, so it can be taken up and degraded by normal hepatocytes. It is thought that biliary obstruction does not lead to an increase in the serum ASGP or delay GSA clearance from the blood, and this was supported by the finding that LHL15 varied within narrow limits after the serum bilirubin decreased in patients with obstructive jaundice due to bile duct carcinoma [28, 29]. While the use of KICG for the evaluation of hepatic function in patients with increased serum bilirubin such as those with obstructive jaundice is problematic, K_L may be used as a substitute for KICG because a good correlation was obtained between KICG and K_L in this study. A value of 0.07 for KICG corresponds to a value of 0.083 for K_L, and a value of 0.06 for KICG corresponds to a value of 0.075 for K_L according to the correlation formula previously described. In two patients in this study, the predicted values of both KICG and K_L were slightly below the above limits, but operation was performed. Postoperative liver dysfunction was severe and prolonged, but the patients did not develop liver failure and recovered. This suggests that the previously described baseline is close to the limit of hepatectomy.

It is concluded that ^{99m}Tc GSA liver scintigraphy is more useful than CT for accurately predicting remnant liver function before hepatectomy based on KICG and for evaluating changes in regional liver function after unilateral occlusion of the portal vein. Moreover, using K_L, it is possible to accurately evaluate liver function in patients with increased serum bilirubin because bilirubin is a competitive inhibitor of ICG, but GSA does not compete with bilirubin.

References

1. Virgolini I, Müller C, Höbart J, et al. Liver function in acute viral hepatitis as determined by a hepatocyte-specific ligand: Tc-99m galactosyl-neogrycoalbumin. *Hepatology* 1992; 15: 593–598.
2. Kudo M, Todo A, Ikekubo K, et al. Quantitative assessment of hepatocellular function through in vivo radioreceptor imaging with technetium 99m galactosyl human serum albumin. *Hepatology* 1993; 17: 814–819.
3. Stadalnik RC, Kudo M, Eckelman WC, et al. In vivo functional imaging using receptor-binding radiopharmaceuticals. *Invest Radiol* 1993; 28: 64–70.
4. Kubota Y, Kitagawa K, Inoue K, et al. Hepatic functional scintigraphic imaging with technetium 99m galactosyl human serum albumin. *Hepatogastroenterology* 1993; 40: 32–36.
5. Inoue I, Machida K, Honda N, et al. Impaired hepatic function in segmental biliary obstruction demonstrated with a receptor-binding radiotracer. *Ann Nucl Med* 1994; 8: 209–212.
6. Higashijima T, Ikeda Y, Koseki M, et al. Changes in ICG Rmax during the course after hepatectomy. *Jpn Pharmacol Ther* 1982; 10: 75–79.
7. Sato S, Mimura H, Noda T, et al. Study for quantitative evaluation of liver volume and accumulation rate of radioactive agent with single photon emission computed tomography. *Radioisotopes* 1987; 36: 265–269.
8. Kawa S, Hazama H, Kojima M, et al. A new liver function test using the asialoglycoprotein-receptor system on the liver cell membrane. *Jpn J Nucl Med* 1986; 23: 907–916.
9. Ohno K, Itoh K, Nagao K, et al. Clinical application of Tc-99m-DTPA-galactosyl serum albumin in hepatobiliary disease. *Jpn J Nucl Med* 1993; 30: 217–224.
10. Nagasue N, Yukaya H, Ogawa Y, et al. Human liver regeneration after major hepatic resection. *Ann Surg* 1987; 206: 30–39.
11. Chen MF, Hwang TL, Hang CF. Human liver regeneration after major hepatectomy. *Ann Surg* 1991; 213: 227–229.
12. Henderson JM, Heymsfield SB, Horowitz J, et al. Measurement of liver and spleen volume by computed tomography. *Radiology* 1981; 141: 525–527.
13. Imaeda T, Kanematsu M, Asada M, et al. Utility of Tc-99m GSA SPET imaging in estimation of functional volume of liver segments in health and liver diseases. *Clin Nucl Med* 1995; 20: 322–328.
14. Kwon AH, Ha-Kawa SK, Uetsuji S, et al. Use of technetium 99m diethylenetriamine-pentaacetic acid-galactosyl-human serum albumin liver scintigraphy in the evaluation of preoperative and postoperative hepatic functional reserve for hepatectomy. *Surgery* 1995; 117: 429–434.
15. Wu J, Ishikawa N, Takeda T, et al. The functional hepatic volume assessed by Tc-99m GSA hepatic scintigraphy. *Ann Nucl Med* 1995; 9: 229–235.
16. Yumoto Y, Umeda M, Oshima K, et al. Estimation of remnant liver function before hepatectomy by means of technetium-99m-diethylenetriamine-pentaacetic acid galactosyl human albumin. *Cancer Chemother Pharmacol* 1994; 33: S1-S6.
17. Kan MK, Hopkins GB. Measurement of liver volume by emission computed tomography. *J Nucl Med* 1979; 20: 514–520.
18. Senda K, Tanaka K, Sakura S. Evaluation of a counting method for liver volume determination using single photon emission computed tomography. *Jpn J Nucl Med* 1984; 21: 279–304.
19. Nakamura K, Maeda H, Nakagawa T, et al. Estimation of total liver uptake and liver uptake per unit of liver volume of Tc-99m (Sn)-*N*-pyridoxyl-5-methyltryptophan (Tc-99m-PMT) using SPET. *Jpn J Nucl Med* 1988; 25: 1363–1369.
20. Ono K, Kato H, Nishibe T, et al. Clinical evolution of hepatic blood flow and liver function with ^{99m}Tc-DTPA-HSA. *Jpn J Surg* 1993; 94: 816–823.
21. Torizuka K, Kawa SKH, Kudo M, et al. Phase III multi-center clinical study on ^{99m}Tc-GSA, a new agent for functional imaging of the liver. *Jpn J Nucl Med* 1992; 29: 159–181.
22. Kudo M, Ikekubo K, Todo A, et al. Clinical utility of receptor imaging in the assessment of liver function. *Jpn J Gastroenterol* 1992; 89: 1349–1359.
23. Shuke N, Aburano T, Nakajima K, et al. The utility of quantitative ^{99m}Tc-GSA liver scintigraphy in the evaluation of hepatic functional reserve: comparison with ^{99m}Tc-PMT and ^{99m}Tc-Sn colloid. *Jpn J Nucl Med* 1992; 29: 573–584.
24. Koizumi K, Uchiyama G, Arai T, et al. A new liver functional study using Tc-99m DTPA-galactosyl human serum albumin: evaluation of the validity of several functional parameters. *Ann Nucl Med* 1992; 6: 83–87.
25. Kudo M, Todo A, Ikekubo K, et al. Receptor index via hepatic asialoglycoprotein receptor imaging: correlation with chronic hepatocellular damage. *Am J Gastroenterol* 1992; 87: 865–870.
26. Kudo M, Todo A, Ikekubo K, et al. Functional hepatic imaging with receptor-binding radiopharmaceutical: clinical potential as a measure of functioning hepatocyte mass. *Gastroenterol Jpn* 1991; 26: 734–741.
27. Yamanaka M, Okamoto E, Toyosaka A, et al. A volumetric study of human liver after intentional occlusion of the unilateral portal vein. *J Jpn Soc Clin Surg* 1985; 46: 532–538.
28. Wu J, Ishikawa N, Takeda T, et al. Evaluation of reserved hepatic function in patients with hepatobiliary tumour by Tc-99m GSA: effect of hyperbilirubinemia and usefulness of regional reserved hepatic functional imaging. *Jpn J Nucl Med* 1996; 33: 161–168.
29. Noguchi T. Studies on functional reserve and resectability of the liver with obstructive jaundice in dogs. *Jpn J Surg* 1979; 80: 931–940.